



## Density functional theory studies of oxygen and carbonate binding to a dicopper patellamide complex

Reza Latifi<sup>a,b</sup>, Mojtaba Bagherzadeh<sup>b</sup>, Bruce F. Milne<sup>c</sup>, Marcel Jaspars<sup>d</sup>, Sam P. de Visser<sup>a,\*</sup>

<sup>a</sup>The Manchester Interdisciplinary Biocenter and The School of Chemical Engineering and Analytical Science, The University of Manchester, 131 Princess Street, Manchester M1 7DN, United Kingdom

<sup>b</sup>Chemistry Department, Sharif University of Technology, P.O. Box 11155-3615, Tehran, Iran

<sup>c</sup>Center for Computational Physics, Department of Physics, University of Coimbra, Rua Larga 3004-516 Coimbra, Portugal

<sup>d</sup>Marine Biodiscovery Centre, Department of Chemistry, University of Aberdeen, Old Aberdeen AB24 3UE, United Kingdom

### ARTICLE INFO

#### Article history:

Received 30 May 2008

Received in revised form 20 August 2008

Accepted 22 August 2008

Available online 2 September 2008

#### Keywords:

Density functional theory

Carbonate

Oxygen

Copper

Tyrosinase

### ABSTRACT

In this work we present results of density functional theory (DFT) calculations on dicopper patellamides and their affinity for molecular oxygen and carbonate. Patellamides are cyclic octapeptides that are produced by a cyanobacterium, and may show promise as therapeutics. Thus, carbonate binding to a dicopper patellamide center gives a stable cyclic octapeptide with a twist of almost 90°. The system exists in close-lying open-shell singlet and triplet spin states with two unpaired electrons in orthogonal  $\sigma^*$  orbitals on each metal center. Subsequently, we replaced carbonate with dioxygen and found a stable  $\text{Cu}_2(\mu\text{-O})_2$  diamond shaped patellamide core. In this structure the original dioxygen bond is significantly weakened to essentially a single bond, which should enable the system to transfer these oxygen atoms to substrates. We predicted the IR and Raman spectra of the  $\text{Cu}_2(\mu\text{-O})_2$  diamond shaped patellamide structure using density functional theory and found a considerable isotope effect on the O–O stretch vibration for  $^{16}\text{O}_2$  versus  $^{18}\text{O}_2$  bound structures. Our studies reveal that carbonate forms an extremely stable complex with dicopper patellamide, but that additional molecular oxygen to this system does not give a potential oxidant. Therefore, it is more likely that carbonate prepares the system for dioxygen binding by folding it into the correct configuration followed in the proposed catalytic cycle by a protonation event preceding dioxygen binding to enable the system to reorganize to form a stable  $\text{Cu}_2(\mu\text{-O})_2$ -patellamide cluster. Alternatively, carbonate may act as an inhibitor that blocks the catalytic activity of the system. It is anticipated that the  $\text{Cu}_2(\mu\text{-O})_2$ -patellamide structure is a potential active oxidant of the dicopper patellamide complex.

Crown Copyright © 2008 Published by Elsevier Inc. All rights reserved.

### 1. Introduction

Dimetal complexes are common features in enzymes and are present, for instance, in ribonucleotide reductase and methane monooxygenase [1–4]. These systems have a dimetal core that is held in position via bridging carboxylate groups and ligated histidine rings. The enzymes bind and utilize molecular oxygen and in the case of methane monooxygenase insert one oxygen atom into a C–H bond of methane; one of the strongest C–H bonds in nature. Although most methane monooxygenase enzymes have a diiron active center there are also a few with a dicopper core [5]. Biomimetic complexes, mimicking the activity of enzyme active-sites, have been synthesized with a dimetal core containing dicopper or diiron and bridging oxo, hydroxo, and peroxy groups [6,7]. These systems have been shown to be very versatile, and for instance, the reaction of an oxoiron nonheme catalyst with another iron nonheme system led to transfer of the oxo group from one

iron system to the other [8]. Nevertheless, recent studies into the oxidative activity of diiron complexes showed that  $\mu$ -oxo- $\mu$ -1,2-peroxy diiron(III) complexes are sluggish oxidants of epoxidation reactions [9]. By contrast a di- $\mu$ -oxo-diiron complex mimicking the active center of methane monooxygenase showed efficient C–H hydroxylation of weak aliphatic bonds [10]. Therefore, understanding the way ligands bind to a dimetal complex and how this influences the electronic and structural features of the complex is important.

Copper containing enzymes have many important functions in nature and function, e.g., as dioxygenases, monooxygenases or oxidases [5,11–15]. Understanding the chemical properties of copper containing enzymes has led to the development of many synthetic analogs or biomimetics [4,16–19]. These systems either have mononuclear or multinuclear copper centers, but in this work we will focus on systems with a binuclear copper center only. Examples of binuclear copper containing enzymes are, for instance, hemocyanin, tyrosinase, and catechol oxidase [20–23]. Thus, tyrosinase enzymes and their biomimetics bind molecular oxygen on a dicopper center to form a  $\mu$ - $\eta^2$ : $\eta^2$ -peroxodicopper(II) complex

\* Corresponding author. Tel.: +44 161 3064882; fax: +44 161 3065201.

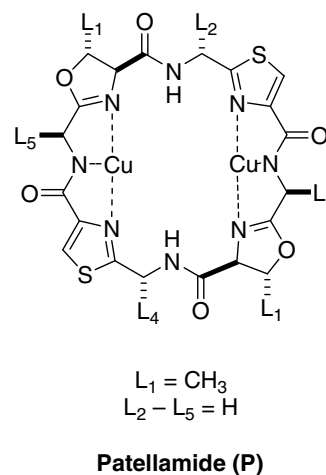
E-mail address: [sam.devisser@manchester.ac.uk](mailto:sam.devisser@manchester.ac.uk) (S.P. de Visser).

that oxidizes phenols to catechol [20,24,25]. Aromatic hydroxylation as performed by tyrosinase enzymes is a challenging process and difficult to achieve due to the strength of the C–H bond.

Biomimetic complexes with a dicopper central core have been extensively studied and their spectroscopic and catalytic properties toward substrates are investigated [26,27]. These systems also bind molecular oxygen and react with substrates via monooxygenase, dioxygenase or tyrosinase type reactions. It has been shown that molecular oxygen either binds as a side-on peroxo or a bis- $\mu$ -oxo dicopper complex [28,29]. Resonance Raman studies of various biomimetic dioxygen bound dicopper complexes gave a wide range of dioxygen stretch vibrations ( $\nu_{\text{OO}}$ ) with values ranging from  $714\text{ cm}^{-1}$  using a PYAN ligand system, PYAN = (N-[2-(4-pyridin-2-yl)-ethyl]-N,N,N'-trimethylpropane-1,3-diamine, while a  $\nu_{\text{OO}}$  of  $817\text{ cm}^{-1}$  was obtained with a TMPA ligand system, TMPA = tris(2-pyridylmethyl)amine [30,31]. Isotopic substitution of molecular oxygen by  $^{18}\text{O}_2$ , however, down-shifted these O–O stretch vibrations considerably with  $-36$  and  $-46\text{ cm}^{-1}$ , respectively, and thereby helps with the characterization of these short-lived species.

Patellamides are cyclic octapeptides that structurally are similar to tyrosinase enzymes because they contain a dicopper core. Due to their small size patellamides have potential in biomimetic studies, but also enables full quantum chemical studies of the real system, whereas full enzyme studies using quantum mechanical or density functional treatment only are currently beyond computational means. These patellamides are, therefore, ideal dicopper complexes for combined theoretical modeling and experimental studies. Patellamides are post-translationally modified ribosomal peptides that are produced by *Prochloron didemni*, the cyanobacterial symbiont of *Lissoclinum patella* (seasquirt) [32,33]. These natural products have been shown to reverse multi-drug resistance in human lymphoblasts [34,35], and as such, these patellamides and their synthetic analogs have potential for commercial exploitation as therapeutics. Recent experimental studies [L. Morris, M. Jaspars, unpublished results] showed patellamides to bind hydrogen peroxide and detoxify it to molecular oxygen via a catalase type mechanism. The experiments, however, seem to be hindered by carbon dioxide in the system, and currently it is unclear whether carbon dioxide assists in the reaction or works as an inhibitor. To ascertain carbonate binding to a dicopper patellamide in the presence of molecular oxygen or hydrogen peroxide, we decided to do a set of DFT calculations that we report here on the properties of patellamides complexed with small molecules, such as  $\text{CO}_3^{2-}$ ,  $\text{O}_2$  and  $\text{H}_2\text{O}_2$ .

The basic structure of patellamides consists of a cyclic octapeptide containing two thiazole and two oxazoline rings (Scheme 1). The structure binds two metal atoms, typically copper atoms although studies of other bound metals have been reported as well [36–40]. The patellamides are split into two classes, symmetric and asymmetric, distinguished from each other by the absence or presence of a phenylalanine residue, respectively. Each patellamide has five characteristic side chains ( $L_1$ – $L_5$ ) that vary among the different patellamides. In addition, it has been shown that patellamide dicopper complexes have an unusual large affinity to carbonate, which has been implicated as being essential for the catalytic properties of the system although it is not clear how and why this is the case [36]. Thus, to find out how carbonate, hydrogen peroxide, water and molecular oxygen coordinate to a dicopper patellamide and how this may influence the intrinsic and putative catalytic properties of the complex we present here results of a density functional theory study on a series of dicopper patellamide models (Scheme 1) with a variety of ligands bound to copper. For simplicity, we have abbreviated all peptide side chains ( $L_2$ – $L_5$ ) to hydrogen atoms and the oxazoline side chains by  $L_1$  = methyl. We show that the dicopper patellamides bind carbonate and dioxygen efficiently and form stable complexes with a rigid structure. Thus, in the diox-



**Scheme 1.** Backbone structure of patellamides (P) in general and the model studied in this work. The side chains  $L_1$ – $L_5$  have been abbreviated to methyl ( $L_1$ ) and hydrogen ( $L_2$ – $L_5$ ) here.

xygen bound structure the O–O bond is considerably weakened and therefore this complex may be an oxidant that transfers one or two oxygen atoms to substrates.

## 2. Methods

All calculations have been performed using established procedures in our group [41,42]. We utilized the unrestricted B3LYP hybrid density functional theory in combination with a double- $\zeta$  quality LANL2DZ basis set on copper that contains a core potential and 6-31G on the rest of the atoms [43–45]. These procedures have been extensively tested and benchmarked against experimental data and shown, e.g., to reproduce rate constants of reaction mechanisms and kinetic isotope effects excellently [46,47]. The structures were fully optimized (without constraints) in the Gaussian-03 program package and a gradient calculation confirmed them as stationary points [48]. All structures have been calculated on the lowest lying singlet and triplet spin states, since it was shown before that transition metal complexes have close-lying spin state structures that lead to multistate reactivity patterns [49–51]. We also tested possible quintet spin states but found them to be considerably higher in energy (by  $60\text{ kcal mol}^{-1}$ ), therefore we did not consider these states further.

We used a dicopper patellamide complex similar to the one shown in Scheme 1 with the side chains of  $L_2$ ,  $L_3$ ,  $L_4$  and  $L_5$  abbreviated to hydrogen atoms. This dicopper patellamide complex had stoichiometry  $\text{Cu}_2\text{C}_{22}\text{H}_{22}\text{N}_8\text{O}_6\text{S}_2$  and was studied with several bound substrates:  $\text{CO}_3^{2-}$ ,  $\text{O}_2$ ,  $\text{H}_2\text{O}_2$  and several water molecules.

Vibrational frequencies reported in this work are taken from the Gaussian-03 frequency calculations of the stationary points and reported without scaling factors. Subsequent reevaluation of the frequencies was done by replacing one or two atoms by a heavier isotope, i.e., replacing bound  $\text{O}_2$  by  $^{18}\text{O}_2$  [52]. The structures with  $^{18}\text{O}_2$  bound were not reoptimized, only the frequencies were recalculated. Infrared (IR) and Raman intensities were taken from the Gaussian frequency outputs and were calculated using standard (default) settings.

## 3. Results

### 3.1. Carbonate binding to a dicopper patellamide complex

It has been anticipated that carbonate binding is essential for the putative catalytic activity of the dicopper patellamides or alter-

natively acts as an inhibitor [36]. To test whether carbonate binding to a dicopper patellamide center gives a stable complex, we set up a dicopper patellamide complex with a carbonate anion and four crystal waters:  $\mathbf{A} = [\text{Cu}_2(\text{H}_2\text{Pat})]^{2+} \cdot \text{CO}_3^{2-} \cdot (\text{H}_2\text{O})_4$ . Optimized geometries of this carbonate-bound patellamide complex in the lowest lying singlet and triplet spin states are shown in Fig. 1. As can be seen the structure is saddle shaped, whereby the carbonate group bridges the two copper ions. Although we included four water molecules in the model that could occupy all vacant ligand positions of the copper atoms, in fact only two water molecules are actually bound to the copper centers: both bind to copper atom Cu2 on the axial and distal sites of the metal. The other two water molecules are uncoordinated but loosely bound due to hydrogen bonding interactions. One of those water molecules bridges the distal bound water molecule of Cu2 with the carbonyl group of the patellamide ring and one of the nitrogen ligands of the other copper center, see Fig. 1. Thus, Cu2 essentially has six-coordination through three nitrogen atoms, two water molecules and the carbonate group. Note that the thiazole and oxazoline groups bound to this copper atom are in an almost planar conformation ( $d_{\text{Cu2NNN}} = 4.2^\circ$  for  $^3\mathbf{A}$  and  $4.3^\circ$  for  $^1\mathbf{A}$ ). This is in sharp contrast to the thiazole and oxazoline groups bound to Cu1 which are strongly bent ( $d_{\text{Cu1NNN}} = 13.1^\circ$  and  $13.2^\circ$  for  $^3\mathbf{A}$  and  $^1\mathbf{A}$ , respectively). In addition, this copper atom has two vacant binding sites, since no water molecules are directly bound there. Note as well that the carbonate ligand is essentially locked in a rigid position through two hydrogen bonding interactions perpendicular to the plane of the carbonate group with two N–H interactions of amide groups on the side of the patellamide. As a consequence, the carbonate group will not be able to rotate and is locked in a very tight binding pattern. These tight binding patterns will put considerable constraint on the structure. The optimized geometries shown in Fig. 1 are in good agreement with crystal structures of similar patellamide systems [36]. For example, the average Cu–N distance of the two copper atoms found here is 2.038 (Cu1) and 2.075 (Cu2) Å, whereas in the crystal structures values of 2.002 and 2.025 Å were obtained [36].

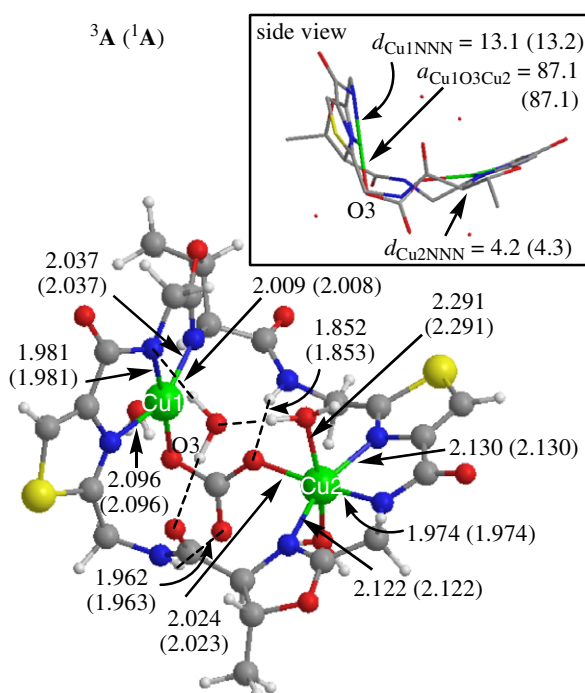


**Fig. 1.** Optimized geometries of  $^3\mathbf{A}$  with bond lengths in Ångstroms and angles ( $a$ ) and dihedral angles ( $d$ ) in degrees. Data in parenthesis refer to the singlet spin state. Color codes: green = Cu, red = O, blue = N, grey = C, yellow = S and white = H.

The electronic ground state of  $\mathbf{A}$  is a system with a degenerate singlet and triplet spin state with the same orbital occupation due to essentially two (non-identical)  $\text{Cu}^{\text{II}}$  centers. The saddle-shaped conformation is a direct result of this orbital occupation. The singly occupied molecular orbitals (Fig. 2) are two  $\sigma^*$  orbitals for the antibonding interactions of the metal with its ligands. In Cu1 the carbonate binds along the molecular  $z$ -axis and interacts via the  $\sigma_{z^2}^*$  (Cu1) orbital. This orbital on Cu2 is virtual as along the axis only weak interactions with water molecules appear. Instead, the singly occupied orbital on Cu2 is of  $\sigma_{x^2-y^2}^*$  type and represents the antibonding interactions of the metal with its ligands. Thus, single occupation of two  $\sigma^*$  orbitals, one along the  $z$ -axis and one in the  $xy$ -plane entices a saddle-shaped geometry on the system. Indeed the Cu2–O3–Cu1 angle (Fig. 1) of  $87.1^\circ$  represents the angle between the  $\sigma_{z^2}^*$  (Cu1) and  $\sigma_{x^2-y^2}^*$  (Cu2) orbitals, so that the saddle-shaped geometry follows the molecular orbital occupation. Since these orbitals are orthogonal and located on different metal centers the interaction of the two unpaired electrons can be ferromagnetically coupled into a triplet spin state or antiferromagnetically coupled into a singlet spin state. As a consequence, these spin states are degenerate ( $\Delta E_{\text{ST}} = 0.0 \text{ kcal mol}^{-1}$ ) in agreement with experimental EPR studies that observed weak ferromagnetic interaction [36]. In mononuclear heme and nonheme oxoiron complexes the degeneracy of spin states of the oxidant can lead to two-state-reactivity patterns with different reaction barriers on each spin state surface [49–51]. Thus, two-state-reactivity can lead to differences in reaction mechanisms with substrates on the individual spin state surfaces. It was shown, for instance, that rearrangement side-reactions of hydroxylation reactions only take place on a high-spin surface, while the low-spin mechanism does not lead to rearrangement [46,53]. Similarly, aldehyde and suicidal by-products in epoxidation reactions were only shown to occur on a high-spin surface and not on the low-spin [54,55].

Subsequently, we removed carbonate from our models and tested four sets of structures: (a) a patellamide without carbonate and copper,  $\mathbf{B1} = (\text{H}_4\text{Pat})$ ; (b) a patellamide without carbonate and copper but with four crystal water molecules,  $\mathbf{B2} = (\text{H}_4\text{Pat}) \cdot (\text{H}_2\text{O})_4$ ; (c) a dicopper patellamide without carbonate,  $\mathbf{B3} = [\text{Cu}_2(\text{H}_2\text{Pat})]^{2+} \cdot (\text{H}_2\text{O})_4$ ; and (d) a dicopper patellamide without carbonate but with six crystal water molecules,  $\mathbf{B4} = [\text{Cu}_2(\text{H}_2\text{Pat})]^{2+} \cdot (\text{H}_2\text{O})_6$ . Full geometry optimizations of these structures were performed and the results are shown in Fig. 3. As is evident from a comparison of the structures shown in Figs. 1 and 3 there are large geometric distortions to the structures due to removal of carbonate. The bare patellamide structure ( $\text{H}_4\text{Pat}$ ,  $\mathbf{B1}$ ) is saddle shaped and close to  $C_2$ -symmetry. The amide groups form hydrogen bonding interactions with the other nitrogen atoms that constrain the geometry. Subsequently, we added four water molecules to this system (structure  $\mathbf{B2}$ ,  $(\text{H}_4\text{Pat}) \cdot (\text{H}_2\text{O})_4$ ) to test the effect of saddling on the patellamide structure in water. As can be seen, the structure is considerably distorted with respect

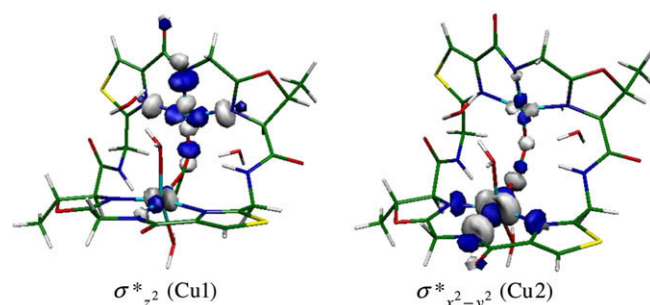


**Fig. 2.** Natural orbitals of  $^3\mathbf{A}$ .

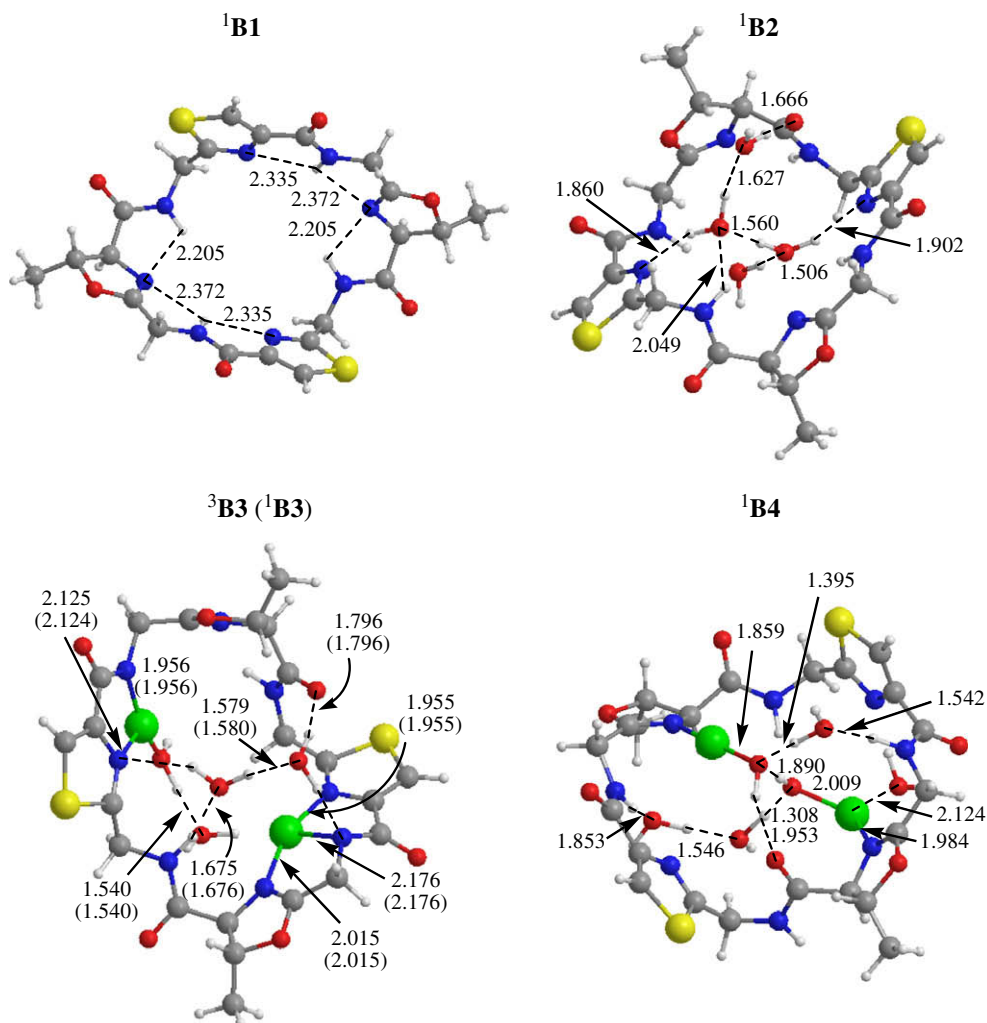


**Fig. 3.** Optimized geometries of patellamide structures without carbonate and or dicopper bound:  ${}^1\mathbf{B1} = [(\text{H}_4\text{Pat})]$ ;  ${}^1\mathbf{B2} = [(\text{H}_4\text{Pat})] \cdot (\text{H}_2\text{O})_4$ ;  ${}^3,{}^1\mathbf{B3} = [\text{Cu}_2(\text{H}_2\text{Pat})]^{2+} \cdot (\text{H}_2\text{O})_4$ ; and  ${}^1\mathbf{B4} = [\text{Cu}_2(\text{H}_2\text{Pat})]^{2+} \cdot (\text{H}_2\text{O})_6$ . All bond lengths in Angstroms. For color coding see Fig. 1.

to structure **B1** mainly due to the fact that the water molecules form hydrogen bonding interactions with the various amide groups. As a result of that the hydrogen bonds between the amide groups, similarly to those in structure **B1**, are broken and replaced with hydrogen bonds with water molecules. Consequently, the patellamide backbone in **B2** is more flexible than it is in **B1** and many close-lying configurations are possible. Moreover, the saddle shape geometry of **B1** is replaced by a chair-like conformation in **B2** similar to that observed in cyclohexane. In a second optimization attempt of structure **B1**, we took the optimized geometry of **B2** and removed all four water molecules. This structure again converged to that shown in Fig. 3 with a saddle conformation due to internal hydrogen bonding interactions.

In structure **B3** the two copper atoms were added to structure **B2** and the system was reoptimized. The most notable difference between **B3** and structure **A** above is the loss of one Cu1–N bond and twisting of the corresponding oxazoline group. Furthermore, the planarity of the ring-systems around Cu2 is distorted and the thiazole group bends downward. In addition, both bound crystal water molecules are released from Cu2 although one water molecule binds to Cu1 instead. As a result, removal of  $\text{CO}_3^{2-}$  from the system changes the coordination of the two copper atoms from hexa- and tetracoordination in **A** to tetra- and tricoordination in **B3**. Finally, the effect of multiple hydrogen bonded water molecules on the dicopper patellamide structures is shown in structure

**B4**, which is  $[\text{Cu}_2(\text{H}_2\text{Pat})]^{2+}(\text{H}_2\text{O})_6$ . Thus, **B3** and **B4** have considerably different geometries so that it is clear that the dicopper patellamide complexes are flexible entities, which change their geometric orientation dependent on the local environment, e.g., through hydrogen bonding interactions with solvent water molecules. Clearly, the system loses considerable flexibility due to binding of carbonate to the dicopper patellamide and a tight molecular geometry is accomplished.

The energy difference (with zero-point energy included) between **A** and isolated carbonate plus **B3** is  $126.6 \text{ kcal mol}^{-1}$ . Therefore, carbonate is strongly bound to the dicopper center via covalent as well as non-covalent (hydrogen bonding) interactions. As follows from the orbital diagram in Fig. 2, the Cu1– $\text{CO}_3^{2-}$  and Cu2– $\text{CO}_3^{2-}$  bonds are not pure covalent bonds but contain significant antibonding character due to the occupation of the  $\sigma_{z_2}^*(\text{Cu1})$  and  $\sigma_{x^2-y^2}^*(\text{Cu2})$  orbitals with one electron. Thus, the Cu1– $\text{CO}_3^{2-}$  bond has three electrons in the  $\sigma_{z_2}$  and  $\sigma_{z_2}^*$  orbitals, while the Cu2– $\text{CO}_3^{2-}$  bond has three electrons in the  $\sigma_{x^2-y^2}$  and  $\sigma_{x^2-y^2}^*$  molecular orbitals. The occupation of  $\sigma_{z_2}(\text{Cu1})^2 \sigma_{x^2-y^2}(\text{Cu2})^2 \sigma_{z_2}(\text{Cu1})^1 \sigma_{x^2-y^2}(\text{Cu2})^1$  formally sums up to approximately one single bond, which agrees well with the bond dissociation energy of carbonate of  $126.6 \text{ kcal mol}^{-1}$ . It may be anticipated therefore, that carbonate binding to the patellamide active site constrains the geometry of the system in anticipation of a catalytic event and will make the system ready for catalysis. Release of carbonate also removes the

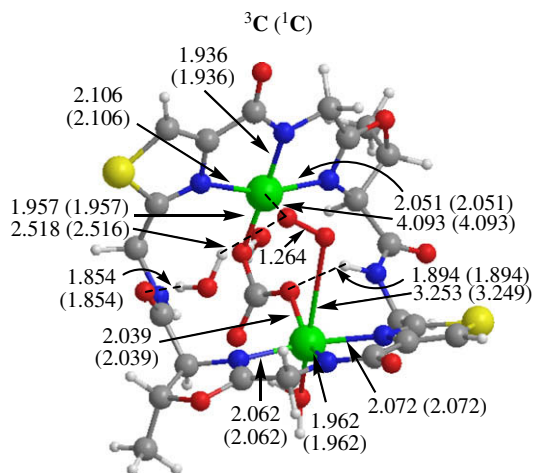


**Fig. 4.** Optimized geometries of  ${}^3\mathbf{1C}$  with bond lengths in Ångströms. Data in parenthesis refer to the singlet spin state. For color coding see Fig. 1.

intramolecular hydrogen bonds of the amide peptide groups, which reorient in **B** and form new hydrogen bonds, with e.g., water molecules. Therefore, release of carbonate from the patellamide opens up the structure and makes it less rigid.

In summary, carbonate binding locks the geometry into a constraint orientation that may enable dioxygen binding or alternatively blocks the catalytic activity as an inhibitor. Carbonate is the ideal ligand to bridge the dicopper center since it gives an almost  $90^\circ$  bend structure that follows orbital occupations, hence the large affinity of patellamides to carbonate as observed experimentally.

### 3.2. Oxygen binding to a dicopper patellamide

The next event in the proposed catalytic mechanism is dioxygen binding to the dicopper patellamide center. Thus, to find out whether dioxygen binds instead of carbonate, i.e., binds to **B3**, or displaces carbonate in structure **A**, we did detailed density functional calculations on possible dioxygen bound complexes. In a first set of calculations we took structure **A** above and replaced one of the water molecules by molecular oxygen to get  ${}^3\mathbf{1C}$   $\mathbf{C} = [\text{Cu}_2(\text{H}_2\text{Pat})]^{2+} \cdot \text{CO}_3^{2-} \cdot \text{O}_2 \cdot (\text{H}_2\text{O})_3$ . Optimized geometries of  ${}^3\mathbf{1C}$  are shown in Fig. 4. Dioxygen is weakly bound via long interactions with the copper ions (4.093 and 3.253 Å in  ${}^3\mathbf{1C}$ ), but is held in position with hydrogen bonding interactions with water molecules. As a consequence of this the replacement of a water molecule in  ${}^3\mathbf{1A}$  by molecular oxygen to give  ${}^3\mathbf{1C}$  is exothermic by  $\Delta E + \text{ZPE} = -1.3 \text{ kcal mol}^{-1}$  only. The triplet spin state is the ground state with the singlet spin state significantly higher in energy (by  $9.4 \text{ kcal mol}^{-1}$ ). The group spin densities predict that a  ${}^3\text{O}_2$  molecule interacts with an open-shell singlet situation on the dicopper centers. The patellamide backbone structure in  ${}^3\mathbf{1C}$  is very similar to that observed for  ${}^3\mathbf{1A}$  above so that addition of molecular oxygen to a patellamide complex with carbonate bound does not change its overall structure.

Obviously, a weak interacting oxygen molecule in hydrogen bonding distance from a dicopper patellamide center is unlikely to be an active oxidant able to perform hydroxylation reactions. Therefore, we tested also an alternative dioxygen bound complex where the two oxygen atoms form a diamond shape with the two copper atoms. The optimized geometries of  $\text{Cu}_2(\mu\text{-O})_2$ -patellamide complex  ${}^3\mathbf{1D}$  ( $\mathbf{D} = [\text{Cu}_2(\text{H}_2\text{Pat})]^{2+} \cdot \text{O}_2$ ) are shown in Fig. 5. The O–O distance is 1.567 (1.582) Å in  ${}^3\mathbf{1D}$  ( ${}^1\mathbf{D}$ ), respectively, which is indicative of a single bond. By contrast, the dicopper distance is

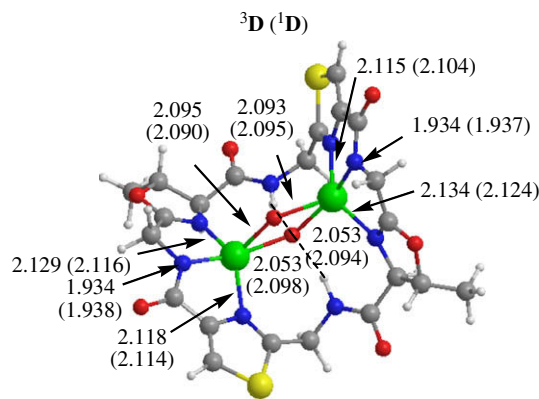


**Fig. 5.** Optimized geometries of  ${}^3\mathbf{1D}$  with bond lengths in Ångströms. Data in parenthesis refer to the singlet spin state. For color coding see Fig. 1.

3.838 (3.878) Å for  ${}^3\mathbf{1D}$  ( ${}^1\mathbf{D}$ ), respectively, while in the carbonate bound structure the distances are 4.569 (4.569) Å for  ${}^3\mathbf{1A}$  ( ${}^1\mathbf{A}$ ). Similarly to the carbonate bound structure, the  $\text{Cu}_2(\mu\text{-O})_2$  patellamide structure is stabilized by two hydrogen bonding interactions between the amide groups and the oxygen atoms. Therefore, a bis- $(\mu\text{-oxo})_2$ -dicopper patellamide is a more compact and stronger bound structure than complexes  ${}^3\mathbf{1C}$  above. Removal of  $\text{O}_2$  from structure  ${}^1\mathbf{D}$  and reoptimization of the rest structure reveals that the bond dissociation energy is  $\Delta E + \text{ZPE} = 37.3 \text{ kcal mol}^{-1}$ .

In contrast to  ${}^3\mathbf{1C}$  above that has a triplet spin ground state, the bis- $(\mu\text{-O})_2$ -dicopper patellamide has an open-shell singlet spin state as ground state. The triplet spin state is  $2.7 \text{ kcal mol}^{-1}$  higher in energy than the open-shell singlet. This is similar to energies obtained recently for a  $\mu\text{-oxo-}\mu\text{-peroxo}$  diiron complex where the electronic ground state was calculated to be an overall open-shell singlet that is built up of the coupling of two sextet spin iron atoms [9]. The spin densities for  ${}^1\mathbf{D}$  are spread out over the copper atoms; one copper atom has spin density of 0.53 and the other has  $-0.53$ , while the two oxygen atoms are closed-shell with negligible spin density. On the other hand, in the triplet spin structure both copper atoms bear similar spin density of 0.56 each, whereas the two oxygen atoms have 0.16 and 0.13 spin density.

To assist experimental identification of critical intermediates in reaction processes, we calculated the IR and Raman spectrum of  ${}^1\mathbf{D}$ , Figs. 6 and 7. The O–O stretch frequency in the  $\text{Cu}_2\text{O}_2$  cluster is located at  $\nu_{\text{OO}} = 760 \text{ cm}^{-1}$ , which is in good agreement with frequencies found for similar dioxo-dicopper complexes but with different ligand systems [13,30,31]. Well lower lying are the

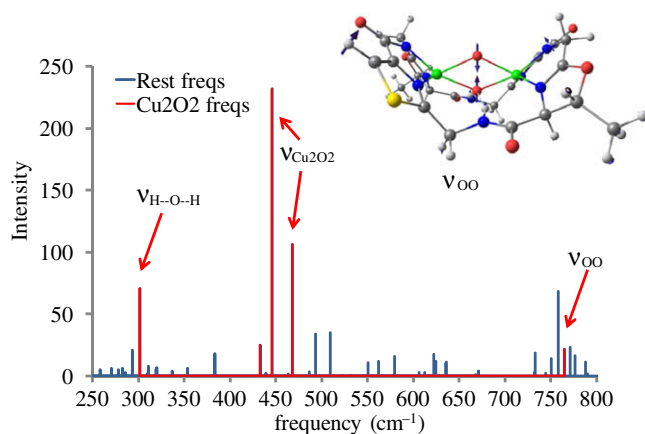


**Fig. 6.** IR vibrational spectrum of  ${}^1\mathbf{D}$  with oxygen sensitive frequencies highlighted in red. The inset shows the vibrational mode of  $\nu_{\text{OO}}$ .

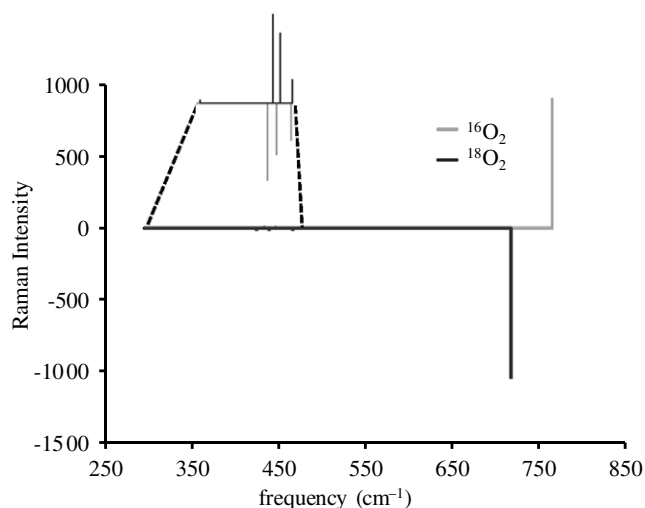


**Fig. 7.** Difference spectrum of **1D** with  $^{16}\text{O}_2$  (positive axis) and **1D** with  $^{18}\text{O}_2$  (negative axis). Raman frequencies calculated with Gaussian and unscaled. The inset shows the region from 300–470  $\text{cm}^{-1}$  enlarged.

symmetrical stretch vibrations of the Cu–O–Cu bonds at around 433–469  $\text{cm}^{-1}$ . Since, one of the oxygen atoms of the  $\text{Cu}_2\text{O}_2$  core is involved in hydrogen bonding interactions with two amide protons of the patellamide backbone, there is also a H–O–H vibration ( $\nu_{\text{H-O-H}} = 302 \text{ cm}^{-1}$ ). It has been shown before that especially an O–O stretch vibration is sensitive to isotopic substitution and replacing  $^{16}\text{O}_2$  by  $^{18}\text{O}_2$  often gives a shift of  $\nu_{\text{O-O}}$  by 30–50  $\text{cm}^{-1}$  in the resonance Raman spectrum [1,2,56,57]. To check the isotopic shift of the oxygen vibrations we further calculated the Raman frequencies of  $^{18}\text{O}_2$  substituted **1D** and compared the frequencies with those for  $^{16}\text{O}_2$ . Note that the Raman intensity for the  $\nu_{\text{O-O}}$  frequency is very large, whereas this band is much less active in the IR spectrum. Moreover, the bending vibrations that give the characteristic lines in the 300–500  $\text{cm}^{-1}$  region in the IR spectrum are almost Raman inactive. Therefore, the IR and Raman spectra give large intensities for different lines that should help with the experimental identification of this particular structure. Isotopic substitution of  $^{16}\text{O}_2$  by  $^{18}\text{O}_2$  shifts the value of  $\nu_{\text{O-O}}$  by  $-43 \text{ cm}^{-1}$ , which is in good agreement with downshifts obtained experimentally for these types of complexes. The three  $\text{Cu}_2\text{O}_2$  vibrations in the 400–

470  $\text{cm}^{-1}$  area only decrease by 2–9  $\text{cm}^{-1}$ . However, as follows from Fig. 7 (and in a similar way from Fig. 6), substitution of  $^{16}\text{O}_2$  by  $^{18}\text{O}_2$  not only affects the value of the vibrational frequencies, but also the magnitude of their intensity. In particular, the O–O stretch vibration has an intensity of 897 in the  $^{16}\text{O}_2$  Raman spectrum, whereas the value has increased to 1038 in the  $^{18}\text{O}_2$  Raman spectrum.

Based on the fact that the diamond shaped  $\text{Cu}_2(\mu\text{-O})_2$  patellamide cluster has long O–O distances with respect to molecular oxygen it may be that the oxygen atoms are transferrable to substrates with low-barriers. Therefore, structure **D** may be a potential oxidant that transfers one of its oxygen atoms to substrates through, e.g., hydroxylation or epoxidation. Thus, recent studies of the catalytic cycles of taurine/ $\alpha$ -ketoglutarate dioxygenase [58,59] and cysteine dioxygenase [60] showed that after dioxygen binding to an iron center, one of the oxygen atoms of  $\text{O}_2$  attacks the substrate to form a ring-structure. Within this ring-structure, the O–O bond is significantly weakened from a conventional double bond to formally a single bond. This step enables a further oxygen transfer reaction with relatively low reaction barriers. It may be anticipated, therefore, that a similar reaction mechanism in dicopper patellamides via the  $\text{Cu}_2(\mu\text{-O})_2$  patellamide complex leads to oxygen atom transfer to substrates. Approach of molecular oxygen to a carbonate bridged dicopper patellamide leads to weak interactions but molecular oxygen is unable to displace carbonate. It may be anticipated, therefore, that a protonation event precedes dioxygen binding or displacement of the carbonate. Combined experimental and theoretical studies in our groups are ongoing to establish this system as an active oxidant in reaction mechanisms.

### 3.3. Hydrogen peroxide binding to a dicopper patellamide

To establish whether a carbonate bridged dicopper patellamide complex would bind hydrogen peroxide efficiently, we set up a model that is based on the features of complex **A** above but with one water molecule replaced by hydrogen peroxide: model **E**  $\text{E} = [\text{Cu}_2(\text{H}_2\text{Pat})]^{2+} \cdot \text{CO}_3^{2-} \cdot \text{H}_2\text{O}_2 \cdot (\text{H}_2\text{O})_3$ . Similarly, to the complexes described above the system appears in close-lying open-shell singlet and triplet spin states that are virtually degenerate. Hydrogen peroxide is not strongly bound to the dicopper center as it does not form a direct bond with one of the metal atoms, Fig. 8. Instead it forms weak (hydrogen bonding) interactions with one of the nitrogen atoms of the patellamide ring and a crystal

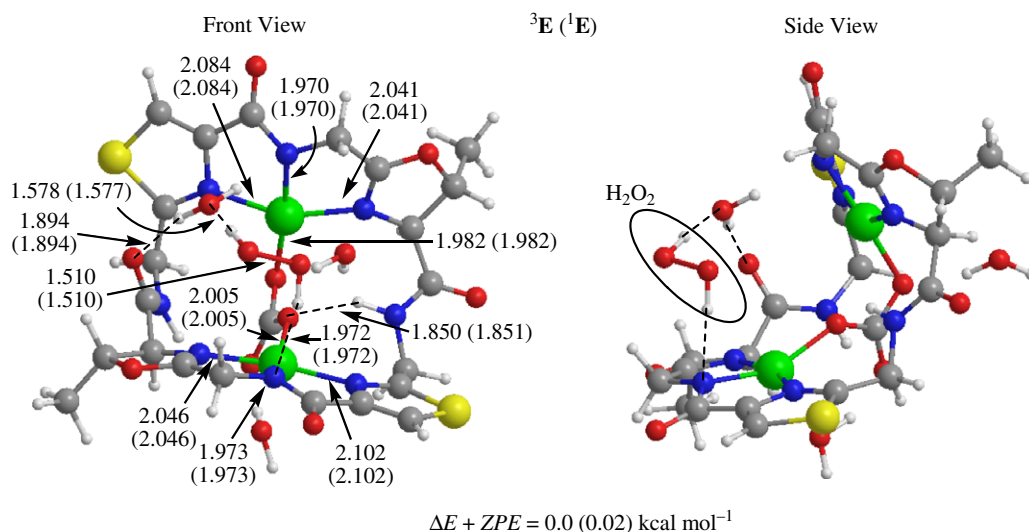


**Fig. 8.** Optimized geometry of  $^3\text{E}$  with bond lengths in Ångströms and relative energies in  $\text{kcal mol}^{-1}$ . Data in parenthesis refer to the singlet spin state. For color coding see Fig. 1.

water molecule. These studies, therefore, suggest that carbonate is too strongly bound to the dicopper patellamide center to establish the dicopper center as an active catalyst and it has to be removed prior to the formation of the active oxidant. Thus, it appears that the most likely function of carbonate is to set up the system for the catalytic event by, e.g., reorienting the structure from the unligated complex **B** to a more constrained geometry as in **A**. However, simply adding molecular oxygen or hydrogen peroxide to this structure does not seem to displace carbonate so that either an electron or proton transfer process will be required to remove carbonate and set up a  $\text{Cu}_2(\mu\text{-O})_2$  active oxidant structure.

#### 4. Summary and conclusions

We present here the first theoretical study on dicopper patellamide structures with bound carbonate, dioxygen, and hydrogen peroxide. The complexes have close-lying spin states and have distinct geometries from the structures without ligands bound. Carbonate binds strongly between two copper centers and folds the patellamide into a perpendicular orientation. This may be necessary for the oxygen activation mechanism and the generation of its active species. Binding of molecular oxygen to the carbonate bridged patellamide structure does not displace carbonate due to the strength of the bonding. Therefore, most likely a protonation or electron transfer process precedes the displacement of carbonate and binding of molecular oxygen to the dicopper center. Further detailed combined experimental and theoretical studies into the full mechanism of catalysis of dicopper patellamides is currently in progress in our groups. Thus, it appears that oxygen activating enzymes come in many different sizes and shapes, whereby the patellamides are the smallest entities while tyrosinase enzymes are much larger. As such the different oxygen activating dicopper enzymes/proteins will have different biotechnological functions and properties. We are just beginning to understand some of their differences but further work is ongoing to find out why nature has developed many different proteins for various functions.

#### 5. Abbreviations

DFT density functional theory

#### Acknowledgements

The National Service of Computational Chemistry Software (NSCCS) is acknowledged for providing CPU time and BBSRC for a Research Development Fellowship to M.J. R.L. thanks the British Council for a scholarship. BFM is the recipient of a post-doctoral Grant (#PTDC/FIS/73578/2006) from the Portuguese Foundation for Science and Technology.

#### Appendix A. Supplementary material

Detailed charges and group spin densities as well as Cartesian coordinates of all structures described in this work are available online. Supplementary data associated with this article can be found, in the online version, at doi:10.1016/j.jinorgbio.2008.08.009.

#### References

- [1] P. Moënne-Loccoz, C. Krebs, K. Herlihy, D.E. Edmondson, E.C. Theil, B.H. Huynh, T.M. Loehr, *Biochemistry* 38 (1999) 5290–5295.
- [2] A.M. Valentine, S.S. Stahl, S.J. Lippard, *J. Am. Chem. Soc.* 121 (1999) 3876–3887.
- [3] E.I. Solomon, T.C. Brunold, M.I. Davis, J.N. Kemsley, S.-K. Lee, N. Lehnert, F. Neese, A.J. Skulan, Y.-S. Yang, J. Zhou, *Chem. Rev.* 100 (2000) 235–349.
- [4] M. Costas, M.P. Mehn, M.P. Jensen, L. Que Jr., *Chem. Rev.* 104 (2004) 939–986.
- [5] L.M. Mirica, X. Ottenwaelder, T.D.P. Stack, *Chem. Rev.* 104 (2004) 1013–1045.
- [6] E. Kim, E.E. Chufán, K. Kamaraj, K.D. Karlin, *Chem. Rev.* 104 (2004) 1077–1133.
- [7] E.E. Chufán, C.N. Verani, S.C. Puiu, E. Rentschler, U. Schatzschneider, C. Incarvito, A.L. Rheingold, K.D. Karlin, *Inorg. Chem.* 46 (2007) 3017–3026.
- [8] C.V. Sastri, K. Oh, Y.J. Lee, M.S. Seo, W. Shin, W. Nam, *Angew. Chem. Int. Ed.* 45 (2006) 3992–3995.
- [9] S.P. de Visser, *Chem. Eur. J.* 14 (2008) 4533–4541.
- [10] G. Xue, D. Wang, R. De Hont, A.T. Fiedler, X. Shan, E. Münck, L. Que Jr., *Proc. Natl. Acad. Sci. USA* 104 (2007) 20713–20718.
- [11] J.P. Klinman, *Chem. Rev.* 96 (1996) 2541–2562.
- [12] M. Fontecave, J.-L. Pierre, *Coord. Chem. Rev.* 170 (1998) 125–140.
- [13] E.I. Solomon, P. Chen, M. Metz, S.-K. Lee, A.E. Palmer, *Angew. Chem. Int. Ed.* 40 (2001) 4570–4590.
- [14] E.I. Solomon, *Inorg. Chem.* 45 (2006) 8012–8025.
- [15] L. Quintanar, C. Stoj, A.B. Taylor, P.J. Hart, D.J. Kosman, E.I. Solomon, *Acc. Chem. Res.* 40 (2007) 445–452.
- [16] A.S. Borovik, *Acc. Chem. Res.* 38 (2005) 54–61.
- [17] W.-D. Woggon, *Acc. Chem. Res.* 38 (2005) 127–136.
- [18] L. Que Jr., *Acc. Chem. Res.* 40 (2007) 493–500.
- [19] W. Nam, *Acc. Chem. Res.* 40 (2007) 522–531.
- [20] K.A. Magnus, H. Ton-That, J.E. Carpenter, *Chem. Rev.* 94 (1994) 727–735.
- [21] C. Gerdemann, C. Eicken, B. Krebs, *Acc. Chem. Res.* 35 (2002) 183–191.
- [22] E.E. Chufán, S.C. Puiu, K.D. Karlin, *Acc. Chem. Res.* 40 (2007) 563–572.
- [23] G. Battaini, A. Granata, E. Monzani, M. Gullotti, L. Casella, *Adv. Inorg. Chem.* 58 (2006) 185–233.
- [24] L.M. Mirica, M. Vance, D.J. Rudd, B. Hedman, K.O. Hodgson, E.I. Solomon, T.D.P. Stack, *Science* 308 (2005) 1890–1892.
- [25] A. Company, S. Palavicini, I. Garcia-Bosch, R. Mas-Ballesté, L. Que Jr., E.V. Rybak-Akimova, L. Casella, X. Ribas, M. Costas, *Chem. Eur. J.* 14 (2008) 3535–3538.
- [26] L.Q. Hatcher, K.D. Karlin, *Adv. Inorg. Chem.* 58 (2006) 131–184.
- [27] E.A. Lewis, W.B. Tolman, *Chem. Rev.* 104 (2004) 1047–1076.
- [28] K.D. Karlin, N. Wei, B. Jung, S. Kaderli, A.D. Zuberbühler, *J. Am. Chem. Soc.* 113 (1991) 5868–5870.
- [29] L. Que Jr., W.B. Tolman, *Angew. Chem. Int. Ed.* 41 (2002) 1114–1137.
- [30] L.Q. Hatcher, M.A. Vance, A.A. Narducci Sarjeant, E.I. Solomon, K.D. Karlin, *Inorg. Chem.* 45 (2006) 3004–3013.
- [31] L.Q. Hatcher, D.-H. Lee, M.A. Vance, A.E. Milligan, R. Sarangi, K.O. Hodgson, B. Hedman, E.I. Solomon, K.D. Karlin, *Inorg. Chem.* 45 (2006) 10055–10057.
- [32] E.W. Schmidt, J.T. Nelson, D.A. Rasko, S. Sudek, J.A. Eisen, M.G. Haygood, *J. Ravel, Proc. Natl. Acad. Sci. USA* 102 (2005) 7315–7320.
- [33] P.F. Long, W.C. Dunlap, C.N. Battershill, M. Jaspars, *Chem. Biol. Chem.* 6 (2005) 1760–1765.
- [34] A.B. Williams, R.S. Jacobs, *Cancer Lett.* 71 (1993) 97–102.
- [35] X. Fu, T. Do, F.J. Schmitz, V. Andrushevich, M.H. Engel, *J. Nat. Prod.* 61 (1998) 1547–1551.
- [36] A.L. van den Brenk, K.A. Byriel, D.P. Fairlie, L.R. Gahan, G.R. Hanson, C.J. Hawkins, A. Jones, C.H.L. Kennard, B. Moubaraki, K.S. Murray, *Inorg. Chem.* 33 (1994) 3549–3557.
- [37] A.L. van den Brenk, D.P. Fairlie, L.R. Gahan, G.R. Hanson, T.W. Hambley, *Inorg. Chem.* 35 (1996) 1095–1100.
- [38] P. Comba, R. Cusack, D.P. Fairlie, L.R. Gahan, G.R. Hanson, U. Kazmaier, A. Ramlow, *Inorg. Chem.* 37 (1998) 6721–6727.
- [39] P.V. Bernhardt, P. Comba, D.P. Fairlie, L.R. Gahan, G.R. Hanson, L. Lötzbeier, *Chem. Eur. J.* 8 (2002) 1527–1536.
- [40] L. Morris, M. Jaspars, J.J. Kettenes van den Bosch, K. Versluis, A.J.R. Heck, S.M. Kelly, N.C. Price, *Tetrahedron* 57 (2001) 3185–3197.
- [41] S.P. de Visser, *J. Am. Chem. Soc.* 128 (2006) 9813–9824.
- [42] S.P. de Visser, *J. Am. Chem. Soc.* 128 (2006) 15809–15818.
- [43] A.D. Becke, *J. Chem. Phys.* 98 (1993) 5648–5652.
- [44] C. Lee, W. Yang, R.G. Parr, *Phys. Rev. B* 37 (1988) 785–789.
- [45] P.J. Hay, W.R. Wadt, *J. Chem. Phys.* 82 (1985) 299–310.
- [46] D. Kumar, S.P. de Visser, P. Sharma, S. Cohen, S. Shaik, *J. Am. Chem. Soc.* 126 (2004) 1907–1920.
- [47] S.P. de Visser, K. Oh, A.-R. Han, W. Nam, *Inorg. Chem.* 46 (2007) 4632–4641.
- [48] M.J. Frisch, G.W. Trucks, H.B. Schlegel, G.E. Scuseria, M.A. Robb, J.R. Cheeseman Jr., J.A. Montgomery, T. Vreven, K.N. Kudin, J.C. Burant, J.M. Millam, S.S. Iyengar, J. Tomasi, V. Barone, B. Mennucci, M. Cossi, G. Scalmani, N. Rega, G.A. Petersson, H. Nakatsuji, M. Hada, M. Ehara, K. Toyota, R. Fukuda, J. Hasegawa, M. Ishida, T. Nakajima, Y. Honda, O. Kitao, N. Nakai, M. Klene, X. Li, J.E. Knox, H.P. Hratchian, J.B. Cross, C. Adamo, J. Jaramillo, R. Gomperts, R.E. Stratmann, O. Yazyev, A.J. Austin, R. Cammi, C. Pomelli, J.W. Ochterski, P.Y. Ayala, K. Morokuma, G.A. Voth, P. Salvador, J.J. Dannenberg, V.G. Zakrzewski, S. Dapprich, A.D. Daniels, M.C. Strain, O. Farkas, D.K. Malick, A.D. Rabuck, K. Raghavachari, J.B. Foresman, J.V. Ortiz, Q. Cui, A.G. Baboul, S. Clifford, J. Cioslowski, B.B. Stefanov, G. Liu, A. Liashenko, P. Piskorz, I. Komaromi, R.L. Martin, D.J. Fox, T. Keith, M.A. Al-Laham, C.Y. Peng, A. Nanayakkara, M. Challacombe, P.M.W. Gill, B. Johnson, W. Chen, M.W. Wong, C. Gonzalez, J.A. Pople, *Gaussian 03, Revision C.01*, Gaussian, Inc., Wallingford, CT, 2004.
- [49] S. Shaik, S.P. de Visser, F. Ogliaro, H. Schwarz, D. Schröder, *Curr. Opin. Chem. Biol.* 6 (2002) 556–567.
- [50] S.P. de Visser, F. Ogliaro, N. Harris, S. Shaik, *J. Am. Chem. Soc.* 123 (2001) 3037–3047.
- [51] S. Shaik, D. Kumar, S.P. de Visser, A. Altun, W. Thiel, *Chem. Rev.* 105 (2005) 2279–2328.
- [52] S.P. de Visser, *Coord. Chem. Rev.* 252 (2008) in press, doi:10.1016/j.ccr.2008.05.001.

- [53] D. Kumar, S.P. de Visser, S. Shaik, *J. Am. Chem. Soc.* 125 (2003) 13024–13025.
- [54] S.P. de Visser, F. Ogliaro, S. Shaik, *Angew. Chem. Int. Ed.* 40 (2001) 2871–2874.
- [55] D. Kumar, S.P. de Visser, S. Shaik, *Chem. Eur. J.* 11 (2005) 2825–2835.
- [56] P. Moënne-Loccoz, J. Baldwin, B.A. Ley, T.M. Loehr, J.M. Bollinger Jr., *Biochemistry* 37 (1998) 14659–14663.
- [57] D.A. Proshlyakov, T.F. Henshaw, G.R. Monterosso, M.J. Ryle, R.P. Hausinger, *J. Am. Chem. Soc.* 126 (2004) 1022–1023.
- [58] T. Borowski, A. Bassan, P.E.M. Siegbahn, *Chem. Eur. J.* 10 (2004) 1031–1041.
- [59] S.P. de Visser, *Chem. Commun.* (2007) 171–173.
- [60] S. Aluri, S.P. de Visser, *J. Am. Chem. Soc.* 129 (2007) 14846–14847.